Biomaterials Science

ROYAL SOCIETY OF CHEMISTRY

PAPER

View Article Online
View Journal | View Issue

Cite this: *Biomater. Sci.*, 2025, **13**, 3561

Development of a bioactive hyaluronic acid hydrogel functionalised with antimicrobial peptides for the treatment of chronic wounds†

Noémie Petit,[a,b] Ana Gomes,[c] Yu-yin Joanne Chang,[a,b] Jessica Da Silva,[d,e,f] Ermelindo C. Leal,[e,f,g] Eugénia Carvalho,[e,f,g] Paula Gomes[c] and Shane Browne *[a,b,h]

Chronic wounds present significant clinical challenges due to delayed healing and high infection risk. This study presents the development and characterisation of acrylated hyaluronic acid (AcHyA) hydrogels functionalised with gelatin (G) and the antimicrobial peptide (AMP) PP4-3.1 to enhance cellular responses while providing antimicrobial activity. AcHyA-G and AcHyA-AMP hydrogels were formed *via* thiol–acrylate crosslinking, enabling *in situ* AcHyA hydrogel formation with stable mechanical properties across varying gelatin concentrations. Biophysical characterisation of AcHyA-G hydrogels showed rapid gelation, elastic behaviour, uniform mesh size, and consistent molecular diffusion across all formulations. Moreover, the presence of gelatin enhanced stability without affecting the hydrogel's degradation kinetics. AcHyA-G hydrogels supported the adhesion and spreading of key cell types involved in wound repair (dermal fibroblasts and endothelial cells), with 0.5% gelatin identified as the optimal effective concentration. Furthermore, the conjugation of the AMP conferred bactericidal activity against *Staphylococcus aureus* and *Escherichia coli*, two of the most prevalent bacterial species found in chronically infected wounds. These results highlight the dual function of AcHyA-AMP hydrogels in promoting cellular responses and antimicrobial activity, offering a promising strategy for chronic wound treatment. Further *in vivo* studies are needed to evaluate their efficacy, including in diabetic foot ulcers.

Received 14th April 2025,
Accepted 19th April 2025

DOI: 10.1039/d5bm00567a

rsc.li/biomaterials-science

Introduction

Chronic wounds pose a significant healthcare challenge, affecting millions worldwide due to impaired healing and a heightened risk of infection.[1–3] Among these, diabetic foot ulcers (DFUs) are a prevalent example, where long-term hyperglycaemia leads to vascular and immune dysfunction, further exacerbating wound chronicity.[4] Other chronic wounds, including venous and pressure ulcers, share similar pathophysiological characteristics, necessitating advanced therapeutic strategies beyond conventional dressings, debridement, and infection management.[4,5] Despite the emergence of novel treatments, their clinical adoption remains limited due to cost constraints and variable efficacy, placing a substantial burden on healthcare systems, caregivers, and patients.[6,7]

Acute wound healing typically follows four sequential and interconnected processes: (1) haemostasis, (2) inflammation, (3) cell proliferation and migration, and (4) matrix deposition and remodelling.[8] Chronic wounds, however, exhibit dysregulation across these phases, particularly impaired angiogenesis, failing to restore tissue vascularity and inhibiting regeneration.[9–11] Biomaterials, and in particular those derived from natural biopolymers, have gained significant attention as potential therapies for chronic wound treatment due to their ability to enhance healing by providing a template that supports cell infiltration and tissue regeneration.[12]

Hydrogels, three-dimensional, crosslinked hydrophilic polymer networks, that can absorb and retain large amounts of water while maintaining their structure have attracted great

[a]*Tissue Engineering Research Group, Department of Anatomy and Regenerative Medicine, Royal College of Surgeons in Ireland, 123, St Stephen's Green, Dublin 2, Ireland. E-mail: shanebrowne@rcsi.ie*
[b]*CÚRAM, Centre for Research in Medical Devices, University of Galway, Galway, H91 W2TY, Ireland*
[c]*LAQV-REQUIMTE, Department of Chemistry and Biochemistry, Faculty of Sciences of the University of Porto, Portugal*
[d]*University of Coimbra, Institute of Interdisciplinary Research, Doctoral Program in Experimental Biology and Biomedicine (PDBEB), 3004-504 Coimbra, Portugal*
[e]*CNC-UC – Center for Neuroscience and Cell Biology, University of Coimbra, 3004-504 Coimbra, Portugal*
[f]*CIBB – Centre for Innovative Biomedicine and Biotechnology, University of Coimbra, 3004-504 Coimbra, Portugal*
[g]*Institute of Interdisciplinary Research, University of Coimbra, 3004-504 Coimbra, Portugal*
[h]*Trinity Centre for Biomedical Engineering, Trinity College Dublin, Dublin 2, Ireland*
† Electronic supplementary information (ESI) available. See DOI: https://doi.org/10.1039/d5bm00567a

interest.[13,14] Hydrogels can maintain a moist wound environment and fill irregularly shaped defects, while also supporting tissue regeneration and providing a protective barrier against microbial infections with the appropriate functionalisation.[15,16] While a vast array of biopolymers have been assessed as hydrogels, hyaluronic acid (HyA) has been identified as particularly suitable due to its biocompatibility, biodegradability, and ease of chemical modification, key criteria in the development of hydrogel-based strategies for tissue repair.[15,17–19] Unlike many native components of the extracellular matrix (ECM), HyA can be chemically modified while preserving its native structure. HyA also promotes fibroblast migration and proliferation, increasing collagen secretion, and contributes to angiogenesis, particularly important given the high amounts of HyA associated with foetal, non-scarring wounds.[15,20–22]

Chemical modification of HyA with acrylate groups (AcHyA) allows for *in situ* hydrogel formation *via* dithiol crosslinkers, as well as the covalent conjugation of thiol-terminated moieties, such as peptides and ECM ligands, to enhance or add further functionality.[23–25] AcHyA hydrogels are highly modular and provide an opportunity to independently modify a range of properties including mechanical properties, degradation, and the availability of cell adhesion ligands.[26,27] With this in mind, we incorporated thiolated gelatin (G) within AcHyA to support cell adhesion and vascularisation. Gelatin is a natural protein derived from collagen and is also biocompatible and biodegradable.[28,29] One main advantage of incorporating gelatin into an AcHyA hydrogel system is the presence of peptide sequences such as RGD and GFOGER in the gelatin which promote cell attachment, fibroblast and endothelial cell growth, aiding in tissue regeneration and vascularisation, all of which are crucial for chronic wound healing.[28–32]

Beyond tissue regeneration, infection remains a major obstacle in chronic wound treatment, where bacterial colonisation sustains inflammation and delays healing.[33,34] While antibiotics remain the standard of care, the rise of antibiotic resistance necessitates alternative approaches. Strategies to combat bacterial infections include (i) addressing antimicrobial resistance mechanisms (*e.g.* RNA silencing, enzyme inhibitors), (ii) enhancing antimicrobial drug delivery, (iii) applying physicochemical inactivation (*e.g.* photoinactivation), and (iv) directly combating antimicrobial resistant bacteria through the use of antimicrobial peptides (AMPs).[35,36] Amongst these alternative strategies, AMPs show great promise as they effectively target both Gram-positive and Gram-negative bacteria and are less prone to induce the development of resistance.[37,38] Furthermore, AMPs can have indirect effects by modulating host immune defences in response to pathogen infection and by enhancing migration and proliferation of cells.[39,40]

However, the clinical application of AMPs is limited due to their poor stability and rapid degradation in protease-rich wound environments, leading to short half-lives and burst release when physically entrapped in biomaterials.[41] To mitigate these limitations, AMPs have been covalently conjugated to biomaterials. While covalent tethering can protect AMPs from enzymatic degradation and limit cytotoxicity, this method can reduce the antimicrobial efficacy of the AMPs due to steric hindrance or restricted mobility.[41] Another challenge in AMP-functionalised biomaterials is the potential loss of antimicrobial efficacy due to structural changes upon conjugation. To overcome this, we engineered a versatile hydrogel based on acrylated hyaluronic acid (AcHyA). This hydrogel is functionalised with thiolated gelatin (AcHyA-G) to enhance cell adhesion and covalently conjugated with a cysteine-terminated AMP (Cys-PP4-3.1) *via* thiol–acrylate Michael addition (AcHyA-AMP). Moreover, we incorporate an Ahx spacer to preserve the AMP's amphipathic nature and optimise its interaction with bacterial membranes. This strategic design maintains antimicrobial potency while minimising steric hindrance. This dual-functional hydrogel provides sustained antimicrobial activity, preventing burst release and improving protease resistance while promoting cell adhesion, all while maintaining the biophysical properties of the hydrogel.[42–44] In this study, we selected PP4-3.1, a hybrid AMP combining the sequences of cosmeceutical pentapeptide-4 (PP4) and a cationic, amphipathic α-helical AMP (3.1), as it effectively disrupts bacterial membranes and inhibits both Gram-positive and Gram-negative bacteria, making it ideal for chronic wound healing applications.[45]

Our approach integrates several key elements: (i) dual functionality through the combination of gelatin for improved cell adhesion and AMPs for sustained antimicrobial effects, (ii) covalent AMP conjugation *via* thiol–acrylate chemistry to ensure controlled release and prolonged antimicrobial efficacy, and (iii) the incorporation of gelatin at minimal concentrations to enhance cell adhesion while preserving the hydrogel's biophysical properties. For this, HyA was modified with acrylate groups to facilitate the conjugation of thiolated gelatin and the cysteine-terminated AMP, *i.e.* Cys-PP4-3.1, while also enabling chemical crosslinking with PEG-dithiol. The effects of gelatin concentration on the biophysical and mechanical properties of AcHyA and AcHyA-G hydrogels were assessed in a concentration-dependent manner, focusing on the optimal formulation to support fibroblast and endothelial cell adhesion and spreading without altering key hydrogel properties. Finally, the antimicrobial activity of the AcHyA-AMP conjugate was evaluated by testing its ability to inhibit the growth of *Staphylococcus aureus* and *Escherichia coli*, bacterial pathogens widely found in non-healing wounds like DFU.[46–49] Ultimately, we aim to develop an AcHyA hydrogel decorated with gelatin and AMPs to enhance the cellular response and reduce the risk of bacterial infection, offering a promising solution for chronic wound treatment.

Materials and methods

Materials

Hyaluronic acid (HyA, sodium salt from *Streptococcus equi*, ~1.5–1.8 MDa), adipic dihydrazide (ADH), 1-hydroxybenzotriazole (HOBt), 1-ethyl-3-[3-(dimethylamino)propyl] carbodiimide

(EDC), dimethyl sulfoxide (DMSO), ethanol, hydrochloric acid (HCl), *N*-acryloxysuccinimide (NAS), thiol-functionalised gelatin, dithiothreitol (DTT), poly(ethylene glycol) dithiol (PEG-dithiol), Coomassie® Brilliant Blue G 250 (Coomassie), hyaluronidase from bovine testes, high glucose Dulbecco's Modified Eagle Medium (DMEM), 1× Dulbecco's phosphate-buffered saline (PBS), Fluorescein isothiocyanate–dextran (70 kDa), Mueller–Hinton Agar, and Mueller–Hinton broth were purchased from Sigma-Aldrich.

Triethanolamine-buffer (TEOA; 0.2 M, pH 8), SnakeSkin™ dialysis membrane (10 000 MWCO), sodium hydroxide (NaOH), 4% paraformaldehyde were purchased from Thermo Fisher Scientific. Hoechst, Alexa Fluor™ 568 Phalloidin, alamarBlue™ were purchased from Invitrogen. Endothelial Cell Growth Medium 2 (EGM-2) was purchased from PromoCell. SB431542 molecule was purchased from TOCRIS.

Unless otherwise specified, concentrations are expressed as % w/v.

Methods

Antimicrobial peptide synthesis. The reference AMP, PP4-3.1 (KTTKSKKLLKWLLKLL-carboxamide) and its Cys-terminated derivative Cys-Ahx-PP4-3.1 were synthesised using solid phase peptide synthesis (SPPS), through the standard Fmoc/*t*Bu orthogonal protection scheme, as previously reported by Gomes *et al.* A cysteine residue (Cys) for chemoselective conjugation to AcHyA through its side chain thiol was added to the *N*-terminus of the peptide, after insertion of a 6-aminohexanoic acid spacer (Ahx) between the additional Cys and the bioactive sequence.[37,45] Final peptide products were identified by electrospray ionization-ion trap mass spectrometry (ESI-IT-MS) and purity was determined by reverse-phase high performance liquid chromatography (RP-HPLC).

Synthesis of acrylate-modified hyaluronic acid (AcHyA). AcHyA was synthesised using previously reported methods.[23–26,50] Briefly, HyA sodium salt (~1.5–1.8 MDa) was reacted with ADH to form hydrazide groups (HyA-ADH), followed by extensive dialysis and ethanol precipitation. HyA-ADH was subsequently reacted with NAS to generate acrylate groups on HyA (AcHyA), followed by extensive dialysis and lyophilisation. The introduction of acrylate groups to HyA was confirmed with ^{1}H NMR.

Synthesis of AcHyA-G and AcHyA-AMP conjugates. AcHyA-G conjugates were synthesised by reacting thiolated gelatin (10 mg) with AcHyA (20 mg) in aqueous solution overnight at room temperature. The conjugates were then extensively dialysed and the purified product was lyophilized and stored at −20 °C until use.

Separately, AcHyA-AMP conjugates were synthesised by reacting AcHyA-G (11.8 mg) conjugates with Cys-Ahx-PP4-3.1 (1 mg) overnight at room temperature. The conjugates were then extensively dialysed and the purified product was lyophilized and stored at −20 °C until use. The conjugation of both gelatin and the AMP to AcHyA were confirmed by ^{1}H NMR.

Hydrogel formation. Hydrogels were prepared with 1.5% AcHyA and varying gelatin concentrations of 0, 0.1, 0.25, and 0.5% (AcHyA-G) (Table 1). For AcHyA-AMP hydrogels, 0.5% gelatin and 0.01% Cys-Ahx-PP4-3.1 were used (Table 1). All conjugates were dissolved in 0.2 M TEOA buffer solution, followed by crosslinking with 1.3% PEG-dithiol.

Table 1 Summary of the hydrogel groups. Concentrations are expressed as % (w/v)

Conjugate	AcHyA	Gelatin	Cys-Ahx-PP4-3.1
AcHyA	1.5	0	0
AcHyA-G	1.5	0	0
		0.1	
		0.25	
		0.5	
AcHyA-AMP	1.5	0.5	0.01

Hydrogel formation was assessed using the vial inversion method, where no flow (no fluidity) indicates successful gelation.[51,52]

Gelatin conjugation and release. The conjugation of thiol-functionalised gelatin to AcHyA was further demonstrated using Coomassie staining. Hydrogels were prepared and allowed to swell in PBS overnight at 37 °C. Following this, the PBS was removed and replaced with 500 µL of 0.1% Coomassie solution. The samples were incubated for 1 h at room temperature while shaking at 100 rpm. The hydrogels were transferred to a de-staining solution, with regular changes made to ensure complete removal of the stain. Finally, the hydrogels were rinsed 3 times in dH_2O, with the last wash used as a blank.

The release of gelatin from the hydrogels was assessed under hydrolytic (PBS) and enzymatic conditions, namely hyaluronidase (HyAse, 10 U mL^{-1}) at 37 °C. At regular intervals, supernatant was collected, and the absorbance was measured at 595 nm. After 48 h of incubation, 1000 U mL^{-1} of HyAse was added to the samples in PBS to ensure complete degradation and gelatin release.

Hydrogel swelling ratio. The swelling properties were evaluated by immersing hydrogels in PBS. Briefly, hydrogels were formed in 24-well plates and weighed after 1 h to obtain the initial mass ($m_{initial}$). PBS was then added in excess to each hydrogel for 24 h at 37 °C, after which the swollen mass ($m_{swollen}$) was measured. The mass swelling ratio (Q_m) was calculated as the ratio of the swollen mass to the initial mass (eqn (1)).

$$Q_m = \frac{m_{swollen}}{m_{initial}} \quad (1)$$

Rheology. The viscoelastic properties (G' and G'') of swollen AcHyA-G and AcHyA-AMP hydrogels were assessed with rheology (HR-1 Discovery Hybrid Rheometer, TA Instruments) using an 8 mm parallel plate geometry. Dynamic time sweeps were performed over 5 min at 37 °C under a constant strain of 0.1% and a frequency of 1 Hz.

Hydrogel degradation. The degradation behaviour of AcHyA-G and AcHyA-AMP hydrogels was assessed under enzymatic and hydrolytic conditions at various pH values. Hydrogels were prepared as previously described and placed in 24-well plates. After gelation, each hydrogel was weighed and

either 10 U mL^{-1} HyAse or buffer (pH 6, 7, or 8) was added. The samples were then incubated at 37 °C, and at regular intervals, the supernatant was collected, and the hydrogels were weighed. The mass loss of the hydrogels was calculated at each time point.

Fluorescence recovery after photobleaching. Fluorescence recovery after photobleaching (FRAP) was conducted to evaluate molecular diffusion within the hydrogel network and provide insight into the mesh size of the material. FRAP measurements were performed on 0% and 0.5% AcHyA-G hydrogels containing fluorescein isothiocyanate (FITC)-dextran (70 kDa, 0.5 mg mL^{-1}). FITC dye was added prior to crosslinking to ensure uniform distribution within the hydrogels. Total fluorescence intensity was measured using a Carl Zeiss LSM 710 confocal microscope with a WPlan-Apochromat 20× (N.A 1.0) objective and an argon laser set at 488 nm. For each hydrogel formulation, three regions of interest were monitored. Initial fluorescence intensity was recorded with 4 prebleach scans at low laser power (0.5%). The selected region was then bleached to approximately 65–70% of the initial intensity using 80% laser power. A total of 150 scans at low power were captured at 2-second intervals to monitor fluorescence recovery. Images were processed using Fiji software.[53]

Mesh size calculation. The mesh size of AcHyA-G hydrogels was calculated using affine and phantom network models, using eqn (2) and (3), respectively.[54,55] Flory interaction parameter χ_1, the molar volume of the solvent (V_1), polymer concentration (c), and polymer functionality (φ) were used to calculate the average MW between crosslinks ($\bar{M}_c$), to then calculate the mesh size (ξ) in eqn (5).[56,57]

$$\frac{1}{M_c\,(\text{affine})} = \frac{2}{M_W} - \frac{\frac{v}{V_1}\left[\ln\left(1-v_{2,s}\right)+v_{2,s}+\chi_1 {v_{2,s}}^2\right]}{v_{2,r}\left[\left(\frac{v_{2,s}}{v_{2,r}}\right)^{1/3}-\frac{1}{2}\left(\frac{v_{2,s}}{v_{2,r}}\right)\right]} \quad (2)$$

$$\bar{M}_c\,(\text{phantom}) = \frac{c\left(1-\frac{2}{\Phi}\right)V_1 {v_{2,r}}^{2/3} {v_{2,s}}^{1/3}}{\ln\left(1-v_{2,s}\right)+v_{2,s}+\chi_1 {v_{2,s}}^2} \quad (3)$$

With the volume fraction of the polymer ($v_{2,r}$) prior to swelling and the volume fraction of the solvent ($v_{2,s}$) after swelling calculated using eqn (4).

$$Q = 1 + \frac{\rho_p}{\rho_s}(Q_m - 1) \quad (4)$$

where ρ_p is the density of the polymer, and ρ_s the density of the solvent.

$$\xi = 0.1748 {M_c}^{1/2} (v_{2,s})^{-1/3} \quad (5)$$

The diffusion coefficient was calculated according to the diffusion model for circular spot using FrapAnalyser Software and is described in eqn (6) and (7).

$$\text{FRAP}\,(t) = a_0 + a_1 \cdot e^{\frac{\tau}{2(t-t_{\text{bleach}})}} \cdot \left(I_0\left(\frac{\tau}{2(t-t_{\text{bleach}})}\right) + I_1\left(\frac{\tau}{2(t-t_{\text{bleach}})}\right)\right) \quad (6)$$

$$\tau = \frac{w^2}{D} \quad (7)$$

$I_0(x)$, $I_1(x)$ are modified Bessel functions, w the radius of bleach spot, D the diffusion coefficient. Two normalising coefficients (a_0, a_1) are introduced to account for the non-zero intensity at bleach moment and incomplete recovery, respectively.[58]

Culture of human dermal fibroblasts and induced pluripotent stem cell-derived endothelial cells. Human dermal fibroblasts (HDFs) from adult donors were purchased from PromoCell, Germany and cultured in DMEM medium containing 10% of Fetal bovine serum (FBS) and 1% penicillin/streptomycin until they reached approximately 80–90% confluence, at which point they were passaged (passage 5–8) and seeded onto AcHyA hydrogels. Vascular cells were differentiated from induced pluripotent stem cells (iPSCs) received from the Harvard Stem Cell Institute, USA (1016 SEVA-line), and endothelial cells (iECs) were purified by magnetic activated cell sorting based on the expression of the endothelial cell surface marker CD31, as previously described.[25] iECs were cultured in supplemented EGM-2 medium (PromoCell, Germany) containing 1% penicillin/streptomycin and 10 μM SB431542, until they reached approximately 80–90% confluence, when they were passaged (passage 2–5) and seeded onto AcHyA hydrogels.

Cell-seeding of hydrogels with human dermal fibroblasts and iPSC-derived endothelial cells. AcHyA hydrogels (100 μL) were prepared in cell culture inserts in a 24-well plate. AcHyA hydrogels were then swollen in PBS for 1 hour at 37 °C and 5% CO_2. HDFs or iECs were then seeded onto AcHyA hydrogels at a density of 30 000 cells per hydrogel in 300 μL of medium. An additional 300 μL of medium was added outside the cell culture inserts. The cell-seeded hydrogels were incubated for 7 days at 37 °C and 5% CO_2.

After 7 days in culture, cell-seeded AcHyA hydrogels were fixed with 4% paraformaldehyde at room temperature for 1 hour and subsequently stained with Phalloidin-Atto 488 (cytoskeleton) and DAPI (nuclei). Imaging was performed using a Carl Zeiss LSM 710 confocal microscope. Images were processed using Fiji software.[53]

Quantification of bFGF protein expression with enzyme-linked immunosorbent assay (ELISA). The release of human basic fibroblast growth factor (bFGF) from HDFs was quantified with ELISA kits (R&D Systems, USA), as per the manufacturer's instructions. Conditioned media was collected on days 3, 5, and 7 post-cell-seeding. Absorbance measurements were taken at 450 and 540 nm, and the expression of bFGF was calculated by extrapolation from the standard curve.

Antimicrobial activity of AcHyA-AMP conjugates. The antimicrobial properties of HyA, AcHyA, and AcHyA-AMP conju-

gates were evaluated against the Gram-positive bacterium *Staphylococcus aureus* (strain Newman) and the Gram-negative bacterium *Escherichia coli* (ATCC 25922).[59] *S. aureus* was cultured overnight in brain heart infusion broth, and the optical density at 600 nm (OD_{600}) was measured, with an OD of approximately 1 corresponding to 1×10^8 colony-forming units (CFU) per mL. *E. coli* was cultured in Mueller–Hinton broth, and OD_{600} measurements were used to estimate CFU mL^{-1} based on the calculation reported by Agilent Genomics.[60] The bacterial broths were then diluted to 1×10^5 CFU mL^{-1} in Mueller–Hinton broth, and 150 μL were added to each sample. A bacterial suspension without any material was prepared as a positive control to assess bacterial growth in the absence of HyA or its derivatives. Samples were incubated at 37 °C, and OD_{600} was monitored over time. After 24 h, 50 μL of each sample were spread onto agar plates and cultured for an additional 24 h, with colony growth recorded by photographing the plates following the incubation period.

Statistical analysis. Data were analysed using GraphPad Prism version 10 (GraphPad Software, La Jolla California USA, https://www.graphpad.com). Statistical significance was determined using one-way or two-way ANOVA ($p < 0.05$), as appropriate, followed by Tukey's *post-hoc* test. An unpaired, two-tailed *t*-test was used to compare two groups ($p < 0.05$). Error bars represent the standard deviation (±SD).

Results and discussion

Chronic wounds, including DFUs, pose a significant clinical challenge due to their prolonged healing times and the high risk of infection, representing a significant burden to patients and healthcare systems worldwide. These wounds are often characterised by excessive inflammation, imbalanced protease activity, and bacterial colonisation, all of which contribute to delayed tissue repair.[5] This study introduces a dual-functional HyA-based hydrogel, combining the bioactivity-enhancing properties of gelatin (AcHyA-G) with the antimicrobial efficacy of the AMP PP4-3.1 (AcHyA-AMP) for chronic wound treatment (Fig. 1). The conjugation of gelatin and PP4-3.1 to AcHyA *via* a thiol–acrylate reaction ensures stable incorporation, enabling controlled release and sustained therapeutic effects at the wound site. These conjugation reactions are achieved using an acrylate-modified HyA which supports hydrogel formation through PEG-dithiol crosslinking, resulting in stable, tuneable mechanical properties.[25] This approach maintains AcHyA's inherent biocompatibility and provides a versatile platform for functionalisation with thiol-containing bioactive molecules, including ECM moieties and peptides, to promote cellular adhesion, activity, and tissue regeneration.[23,24,50] The incorporation of gelatin into the AcHyA matrix enhances cell adhesion, while the incorporation of AMPs offers an effective strategy for infection prevention, ultimately supporting tissue regeneration and improving wound healing.[61–66]

The degree of modification of HyA with acrylate groups (AcHyA) was assessed by proton NMR. The presence of two peaks in the 5.5–6.5 ppm region confirmed the successful introduction of acrylate groups onto HyA, with a modification degree of approximately 25%, consistent with previous reports (Fig. 2A).[25] The acrylate-thiol reaction was then leveraged to conjugate thiol-functionalised gelatin and the Cys-terminated AMP, PP4-3.1, to AcHyA. A subsequent decrease in the degree of modification to 12% (gelatin, Fig. 2A) and 9.5% (PP4-3.1, Fig. S1†) suggested that fewer acrylate groups were detectable due to their consumption by the conjugation of both gelatin and PP4-3.1 to AcHyA.

PEG-dithiol was used to crosslink the AcHyA hydrogels *via* a thiol–acrylate reaction between the acrylate groups of AcHyA and thiol groups in PEG-dithiol.[67] PEG-dithiol has demonstrated its biocompatibility and non-immunogenic nature, with minimal risk of an inflammatory response.[68–70] Having established the role of PEG-dithiol in crosslinking, we used the protein-specific dye Coomassie to further confirm the conjugation of gelatin to AcHyA to produce AcHyA-G (Fig. 2B and C). We tested gelatin concentrations up to 0.5%, focusing on identifying the optimal concentration required to enhance cellular

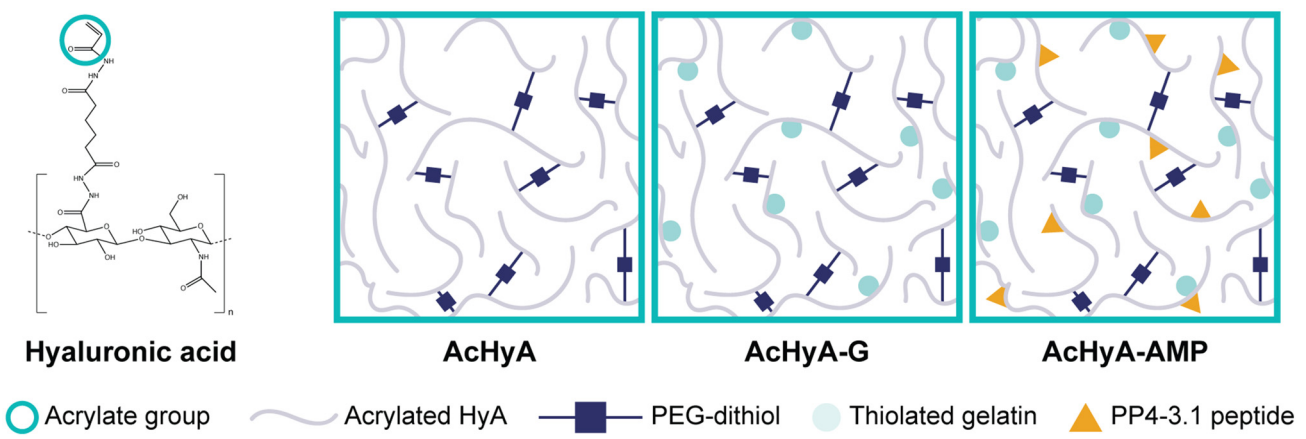

Fig. 1 Schematic representation of the functionalised HyA hydrogels. HyA hydrogels are composed of acrylated HyA chains (AcHyA) along with AcHyA functionalised with thiolated gelatin (AcHyA-G) and PP4-3.1 antimicrobial peptide (AcHyA-AMP), and crosslinked with PEG-dithiol.

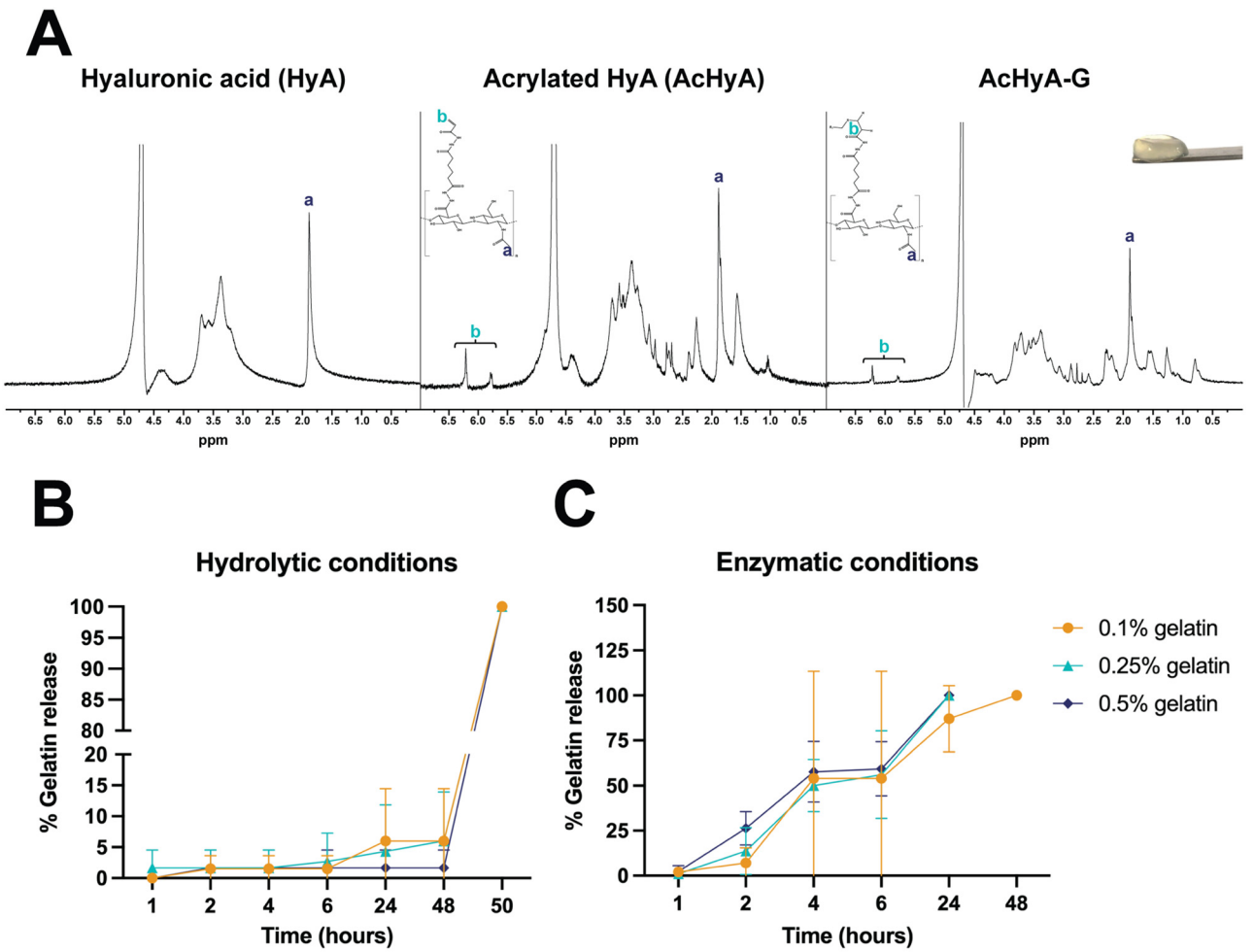

Fig. 2 Development and characterisation of AcHyA hydrogels functionalised with gelatin. (A) ^{1}H NMR was used to confirm the modification of HyA with acrylate groups and the conjugation of thiolated gelatin (AcHyA-G). A representative image of an AcHyA hydrogel functionalised with gelatin is shown. (B) The release of gelatin from HyA hydrogels was assessed in hydrolytic conditions (PBS) with the addition of 1000 U mL^{-1} HyAse at 48 h, and (C) in enzymatic conditions (10 U mL^{-1} HyAse). Data represents mean ± SD (n = 3). Analysis performed using two-way ANOVA; $p < 0.05$.

adhesion while maintaining biophysical properties. Minimal to no gelatin release occurred from AcHyA hydrogels in PBS over the 48 h study period, indicating that gelatin was covalently conjugated to AcHyA *via* acrylate–thiol bonds. The addition of HyAse at the 48 h timepoint cleaved the β-1,4-glycosidic bonds between the HyA subunits, facilitating AcHyA hydrogel degradation and resulted in rapid gelatin release (Fig. 2B). In the presence of a lower concentration of HyAse, 10 U mL^{-1}, gelatin release was more gradual and complete within 48 h, demonstrating steady release of gelatin as the AcHyA hydrogel degraded (Fig. 2C). This emphasises that gelatin is stably conjugated to the AcHyA hydrogel, with release facilitated only by degradation of the AcHyA hydrogel, in this case mediated by the addition of HyAse.

The impact of gelatin incorporation on the mechanical properties of AcHyA hydrogels was evaluated using rheology. First, the gelation time was observed with the vial inversion method, where no flow was observed after 5 min of incubation for AcHyA hydrogels with and without gelatin, implying rapid crosslinking and hydrogel formation (Fig. 3A). The storage moduli obtained were 928 ± 137, 995 ± 221, 1234 ± 78, and 1210 ± 136 Pa for 0%, 0.1%, 0.25%, and 0.5% gelatin samples, respectively (Fig. 3B). However, no statistically significant differences were observed between samples, demonstrating that the mechanical properties of AcHyA-G hydrogels were independent of gelatin concentration. Next, we investigated the influence of gelatin concentration on the swelling behaviour of the hydrogels to evaluate their moisture retention ability. After 24 h in PBS, AcHyA hydrogels of varying gelatin concentrations swelled to approximately 150%, with no statistically significant differences observed between groups; this indicates that the swelling properties of AcHyA were not affected by gelatin incorporation at concentrations up to 0.5% (Fig. 3C). These findings suggest that gelatin incorporation into AcHyA hydrogels does not significantly alter their mechanical or swelling properties.

We assessed the stability of AcHyA-G hydrogels at various pH values with and without the addition of HyAse enzyme to

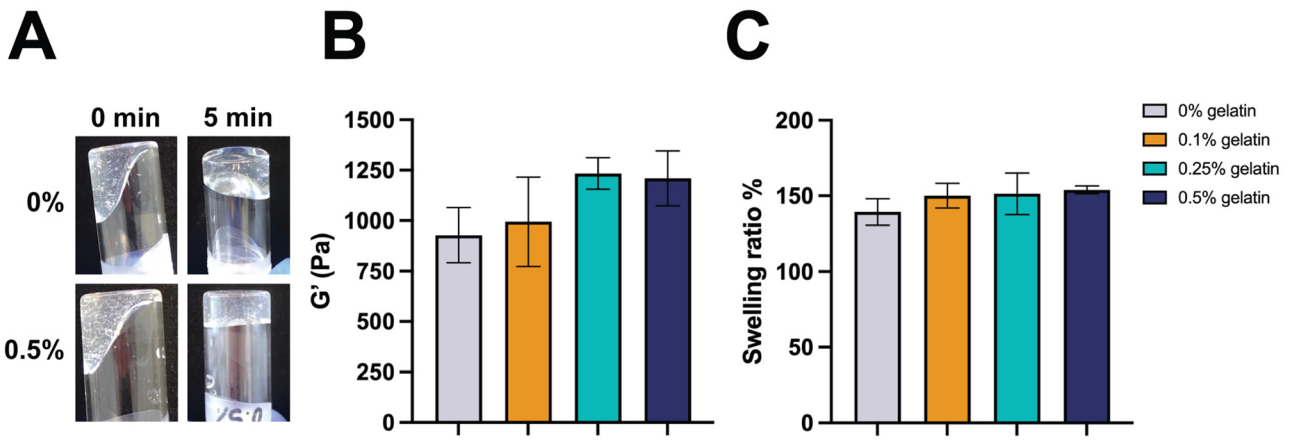

Fig. 3 Gelatin incorporation does not significantly affect the mechanical properties or swelling behaviour of AcHyA hydrogels. Characterisation of HyA-derived hydrogels (A) gelation time was assessed with the inversion method for the 0% (top lane) and 0.5% (bottom lane) gelatin formulations, (B) storage modulus, and (C) swelling ratio. Data represents mean ± SD (n = 3). Analysis performed using one-way ANOVA; $p < 0.05$.

assess suitability in the wound environment. The following pH values were chosen to simulate various wound conditions: epithelialized wounds (pH 6), neutral environments (pH 7), and alkaline chronic wounds (pH 8).[71] Under hydrolytic conditions, minimal degradation was detected across all conditions. In fact, gelatin-containing hydrogels swelled to a maximum of 130% at pH 6 (Fig. 4A), 125% at pH 7 (Fig. 4B), and 133% at pH 8 (Fig. 4C). In contrast, the 0% gelatin sample only swelled under neutral conditions, losing approximately 20% of its original mass at both pH 6 and pH 8. The differences between the gelatin-containing and gelatin-free samples were pronounced, especially in simulated epithelialized and

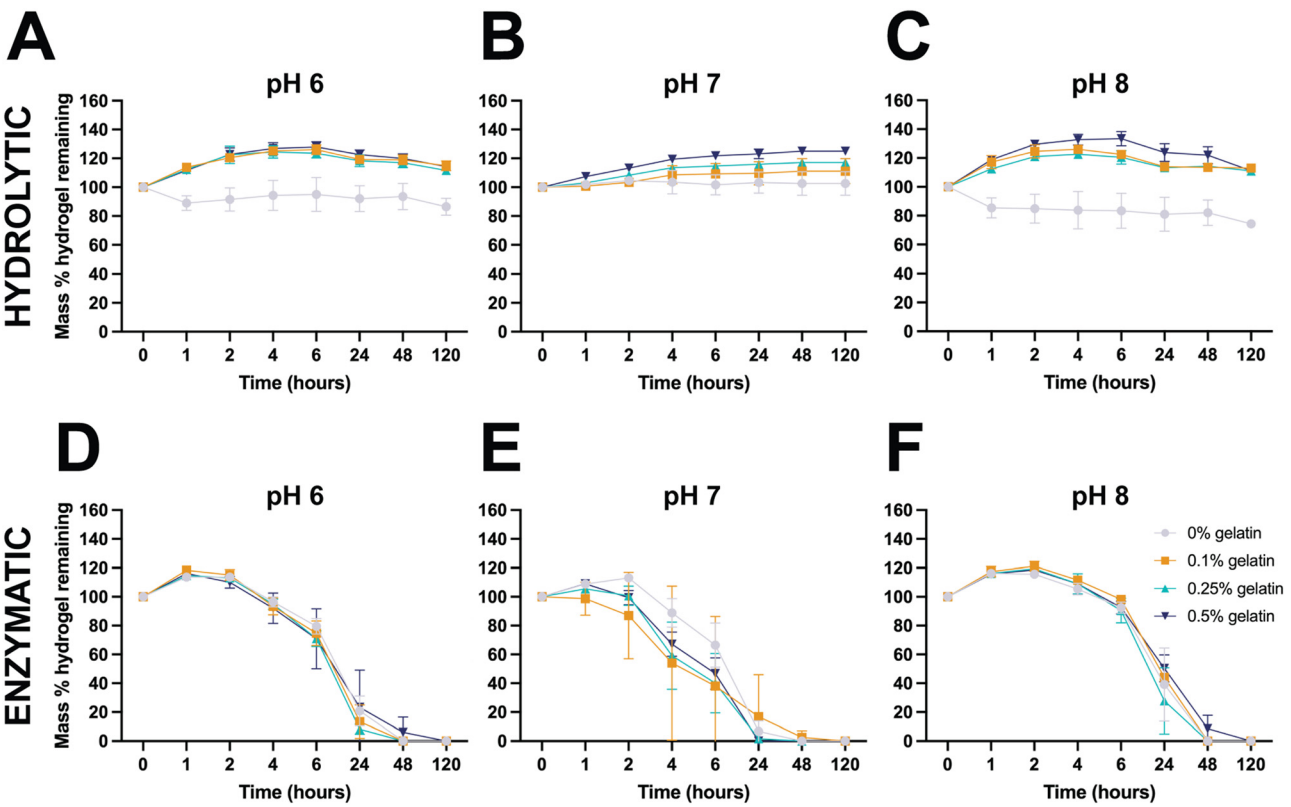

Fig. 4 Gelatin incorporation improves stability of AcHyA hydrogels under varying physiological conditions. Characterisation of HyA-derived hydrogels (A–C) hydrolytic degradation (PBS), and (D–F) enzymatic degradation (10 U mL^{-1} HyAse). Data represents mean ± SD (n = 3). Analysis performed using two-way ANOVA; $p < 0.05$.

alkaline wound conditions after 5 days, indicating the enhanced suitability of AcHyA-G hydrogels in the compromised wound environment (Fig. 4A and C). Throughout the study, the 0% and 0.5% samples remained statistically different (Fig. 4A and C). At pH 7, the presence of gelatin had a negligible effect at early time points (1 and 2 h), and all hydrogels remained stable over 5 days (Fig. 4B). This data demonstrates the stability of AcHyA-G hydrogels, and their suitability for exudate absorption, with gelatin enhancing their capacity to maintain a moist environment.

In addition to hydrolytic degradation, understanding enzymatically-mediated degradation kinetics of wound dressings is crucial as it significantly influences cell and tissue responses, essential for effective wound healing applications.[16,72] The controlled degradation of hydrogels is essential for coordinating cell-mediated remodelling with tissue regeneration, supporting effective cell infiltration and vascularisation within the wound site.[24] Optimally tuned degradation rates can enhance wound healing by promoting timely cell migration, angiogenesis, and ECM deposition.[73–75] During healing, cells secrete a range of enzymes, including HyAse and matrix metalloproteinases (MMPs), that contribute to these processes. Therefore, hydrogels should exhibit a degradation rate that supports cell infiltration and matches the rate of neotissue formation. AcHyA-G hydrogels are susceptible to enzymatic degradation by HyAse, present in the wound environment, making it essential to assess their degradation rates to ensure they maintain integrity while promoting healing.[76] Initially, all hydrogels exhibited swelling within the first few hours, likely due to a reduced overall cross-linking density in the hydrogel network as a result of initial degradation.[25,77] However, both AcHyA and AcHyA-G hydrogels gradually degraded over 5 days across all pH levels. After 24 h at pH 6 (Fig. 4D) and pH 7 (Fig. 4E), all hydrogels underwent significant degradation, with the mass dropping to approximately one-fifth of the original mass, likely due to increased HyAse activity in these conditions. At pH 8, all hydrogels maintained about 50% of their mass for approximately 24 hours (Fig. 4F). However, across all pH levels, the degradation profiles were not statistically different. These findings indicate that AcHyA-G hydrogels remain susceptible to HyAse-mediated degradation, essential for supporting wound healing, and that the incorporation of gelatin does not significantly impact the overall degradation kinetics. Instead, it enhances hydrogel swelling and moisture retention capabilities without compromising structural integrity. This suggests that AcHyA-G hydrogels are effective in maintaining their properties and remaining biodegradable under the simulated wound conditions assessed.

To further explore the structural characteristics of AcHyA hydrogels and the impact of gelatin incorporation, we calculated the mesh size, which represents the distance between cross-links or physical entanglements within the polymer network. The mesh size is a critical parameter as it directly affects molecular diffusion, material stiffness, degradation kinetics, and cell–material interactions.[25,78] Furthermore, in therapeutically loaded hydrogels, the mesh size plays a role in the retention or release rate of therapeutic molecules, including AMPs, as they may be cleaved by native enzymes. Thus, mesh size is a critical parameter in assessing therapeutic release kinetics as well as ensuring sufficient nutrient transport to support the viability of invading cells.[79,80] Mesh size may be altered by adjusting crosslinking density and HyA molecular weight (MW) which modifies the number of chemical and physical crosslinks, including chain entanglements.[25,81,82] The mesh size of AcHyA (0% gelatin) and AcHyA-G (0.5% gelatin) hydrogels were estimated using both the Phantom network and Affine network models based on the storage modulus (G') (Fig. 5A and B). The Phantom model yielded mesh sizes on the order of 80–90 nm, while the Affine model estimated mesh sizes of approximately 110–130 nm, with no statistical difference detected between groups regardless of gelatin concentration (Fig. 5A and B). These values are consistent with previously reported measurements, and confirm the formation of a nanoporous hydrogel network.[83,84]

FRAP was employed as a technique to assess molecular mobility and diffusion within the 0% and 0.5% AcHyA-G hydrogels, (Fig. 5C and D). FITC-dextran (70 kDa) was used as a representative biomolecule to assess the molecular diffusion of nutrients and other bioactive molecules through AcHyA hydrogels. FITC-Dextran loaded hydrogels were bleached to approximately 65–70% of their initial fluorescence, and the fluorescence recovery was monitored for 300 s post-bleaching as unbleached molecules diffused back into the region of interest (Fig. 5C and D).[85,86] Both AcHyA and AcHyA-G hydrogel formulations, regardless of the presence of gelatin, demonstrated a rapid recovery of fluorescence, reaching 90% of initial intensity within the first 60 seconds and nearly complete recovery by the end of the 300 seconds, indicative of a mobile fraction φ_{mob} of 1.[87] This rapid recovery of fluorescence indicates a dominant mobile phase favourable for molecular transport and release from the AcHyA and AcHyA-G hydrogels.[26] Diffusion coefficients were calculated to be around 0.5 $\mu m^2\ s^{-1}$ for both samples, with no significant difference detected between them. This aligns with data from HyA-based hydrogels, which report diffusion coefficients for smaller FITC-dextran (4 kDa) and mesh sizes ranging from 0.66 to 1.06 $\mu m^2\ s^{-1}$.[87] The similar recovery dynamics and molecular release profiles demonstrated between groups revealed that there is no impact of the incorporation of gelatin in AcHyA hydrogels on molecular diffusion. Additionally, the complete fluorescence recovery indicates a mobile fraction allowing molecules with MW up to 70 kDa to readily diffuse within the AcHyA-G hydrogel network. In contrast, hydrogels with incomplete fluorescence recovery indicate immobile fractions ($\varphi_{mob} < 1$), where molecules become trapped within the network, as demonstrated in HyA-based hydrogels loaded with varying dye charges.[87] With a MW of 1940.5 Da, PP4-3.1 peptide would be expected to readily diffuse through and indeed out of the AcHyA-G hydrogels. However, since it is directly conjugated to AcHyA-G by thiol–acrylate reaction, it is therefore not free to diffuse through the hydrogel network. Instead, its release is

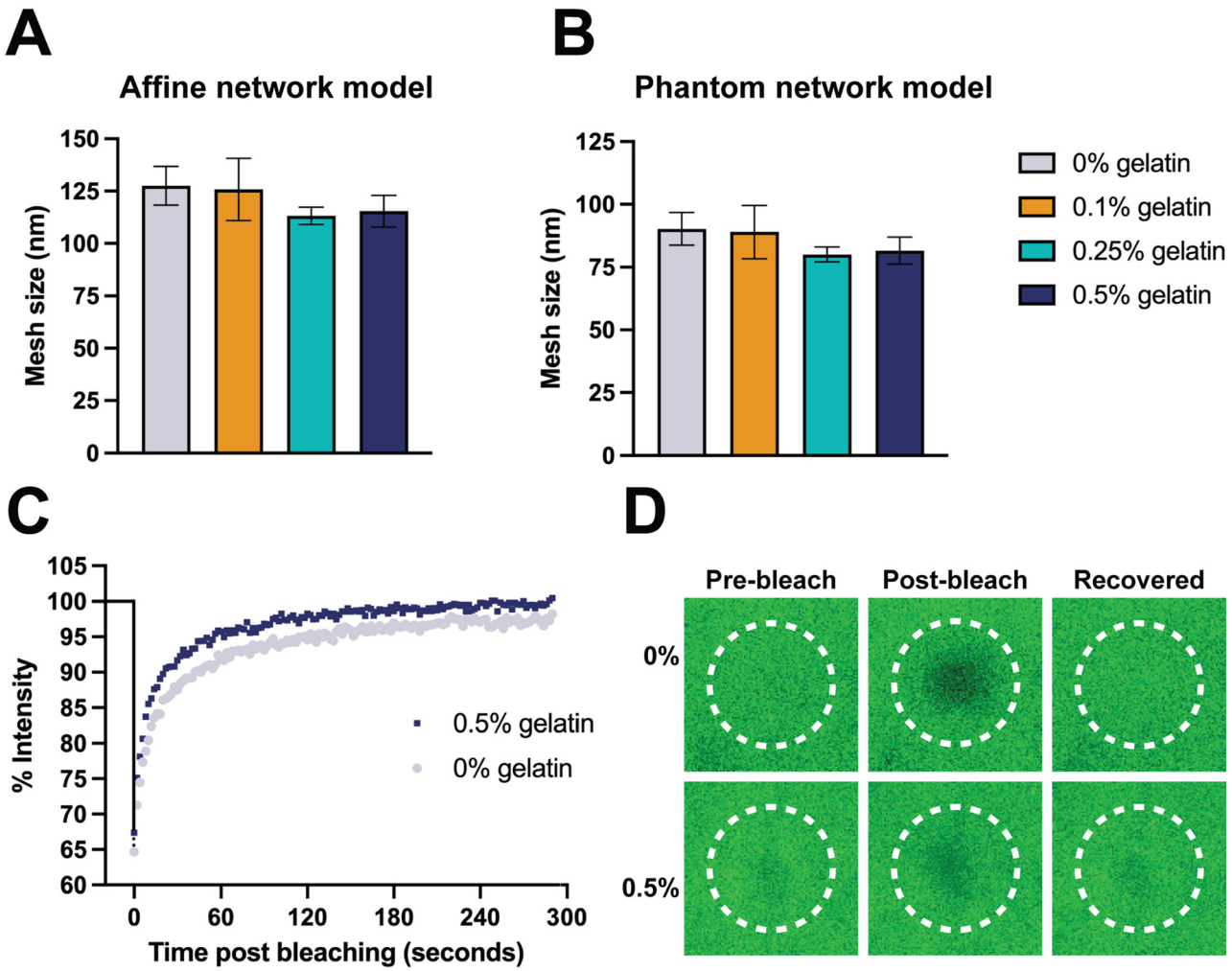

Fig. 5 Gelatin concentration has minimal impact on mesh size and molecular diffusion in AcHyA hydrogels. Mesh size was calculated using (A) affine and (B) phantom network models. (C) Recovery of fluorescence after photobleaching with 0% and 0.5% gelatin hydrogels incubated with 70 kDa FITC-Dextran and (D) confocal images of the bleached spot during treatment. Data represents mean ± SD (n = 3). Analysis performed using one-way ANOVA; $p < 0.05$.

anticipated to occur only upon degradation of the hydrogel, similar to the behaviour observed with conjugated gelatin (Fig. 2B and C). Furthermore, our results align with the calculated mesh sizes, as expected since the molecular diffusivity is inherently correlated with the hydrogel mesh size, which was similar for both 0% and 0.5% gelatin AcHyA hydrogels (Fig. 5A and B). These results can also be correlated with the degradation observed in Fig. 4D–F, since the mesh size and molecular diffusion were found to be similar across the groups, this means similar diffusion of degrading enzymes (*i.e.* HyAse) and access to target cleavage sites throughout the hydrogel network.[88,89] Overall, molecular mobility and diffusion appeared independent of the gelatin concentrations used in this study, with both AcHyA and AcHyA-G hydrogel formulations demonstrating comparable molecular dynamics. This characteristic is of important consideration since it allows for independent tuning and optimising of the AcHyA-G hydrogel's biophysical and biological properties. Gelatin incorporation did not significantly alter the biophysical properties of AcHyA hydrogels in this study, for several possible reasons. The MW of gelatin used in this study is relatively small (50–100 kDa) compared to the MW of HyA used to form the hydrogel system (1.5 MDa). In addition, the relatively low concentrations of gelatin incorporated (≤0.5%) may not have been sufficient to create significant changes in the hydrogel's mechanical properties. The impact of gelatin on the hydrogel structure is likely dependent on both the concentration and MW of the gelatin, with higher MW or greater gelatin concentrations potentially leading to stronger molecular interactions and greater alterations in stiffness or elasticity.[90] In our hydrogel system, the selected formulations allowed for the introduction of biochemical cues without affecting the overall physical properties of the AcHyA hydrogel.

To enhance bioactivity and support cellular adhesion, thiolated gelatin was incorporated into the AcHyA hydrogel. Gelatin, derived from the hydrolysis of collagen, is biocompati-

ble, biodegradable, and contains key peptide sequences known to promote cell adhesion. These sequences, particularly the RGD motif, interact with integrins such as α5β1, α4β1, and αvβ3, which are involved in regulating cell activity, including adhesion, proliferation, and migration.[91] By varying the concentration of gelatin, we aimed to tune the cellular response and optimise AcHyA hydrogel composition to support adhesion and spreading of dermal fibroblasts (HDFs) and endothelial cells (iECs) – two critical cell types involved in wound repair and vascularisation.[92] As shown in Fig. 6A, gelatin concentration significantly influenced the morphology and behaviour of the HDFs. Lower gelatin concentrations led to fewer, rounded cells, suggesting poor adhesion and limited cell spreading. In contrast, higher gelatin concentrations resulted in enhanced cell spreading and elongation, demonstrating improved adhesion of HDFs. The average cumulative cell area also varied across all formulations: 159.2 ± 869.6, 9901.7 ± 5341.5, 7476.6 ± 1415.3, and 11 240.4 ± 3140.2 μm^2 for 0%, 0.1%, 0.25%, and 0.5% gelatin formulations, respectively (Fig. 6B). Moreover, the presence of stress fibres in the 0.1%, 0.25%, and 0.5% gelatin formulations indicated that fibroblasts were able to establish cell–matrix interactions (Fig. 6A).[93] A similar pattern was observed in iECs (Fig. 6C), albeit with a greater level of cell coverage, where higher gelatin concentrations facilitated the adhesion of a greater number of iECs and the formation of dense cellular networks with greater cell spreading, while lower concentrations of gelatin showed fewer iECs, and minimal network formation. This was evidenced by the average cumulative cell area which ranged from 428.8 ± 294.1, 31 813.6 ± 26 166.6, 31 149.5 ± 15 072.8, 27 280.2 ± 4778.2 μm^2 for 0%, 0.1%, 0.25%, and 0.5% gelatin formulations, respectively (Fig. 6D).

To assess fibroblast bioactivity, we quantified the secretion of bFGF, an essential growth factor involved in tissue repair and angiogenesis.[94] bFGF plays a critical role in stimulating fibroblast proliferation, ECM deposition, and tissue regeneration, while also promoting angiogenesis indirectly by activating endothelial cells.[95,96] By day 3, bFGF levels varied across all conditions, ranging from 2.32 ± 2.06 pg mL^{-1} (0.1% gelatin) to 4.17 ± 3.88 pg mL^{-1} (0.5% gelatin). This decline persisted through day 5, with bFGF levels remaining low in all groups. However, by day 7, bFGF secretion increased again in the 0.5% gelatin formulation (8.54 ± 1.51 pg mL^{-1}), suggesting that higher gelatin content sustains fibroblast activation over time. This increase in bFGF secretion aligns with the improved fibroblast adhesion and spreading observed in the imaging analysis (Fig. 7), reinforcing the role of gelatin in supporting cellular engagement with the hydrogel matrix.

These results suggest that gelatin concentration influences HDFs and iECs behaviour in a concentration-dependent manner. HyA, though known to support cell proliferation, lacks integrin-binding sites, which are essential for cell adhesion.[16,97] This absence, combined with the fact that cells were seeded on top of the AcHyA hydrogels rather than encapsulated within them, likely contributed to the poor attachment observed in gelatin-free AcHyA hydrogels. In contrast, the RGD motifs in gelatin enhanced HDF and iEC adhesion and migration.[98,99] Our results are consistent with previous studies

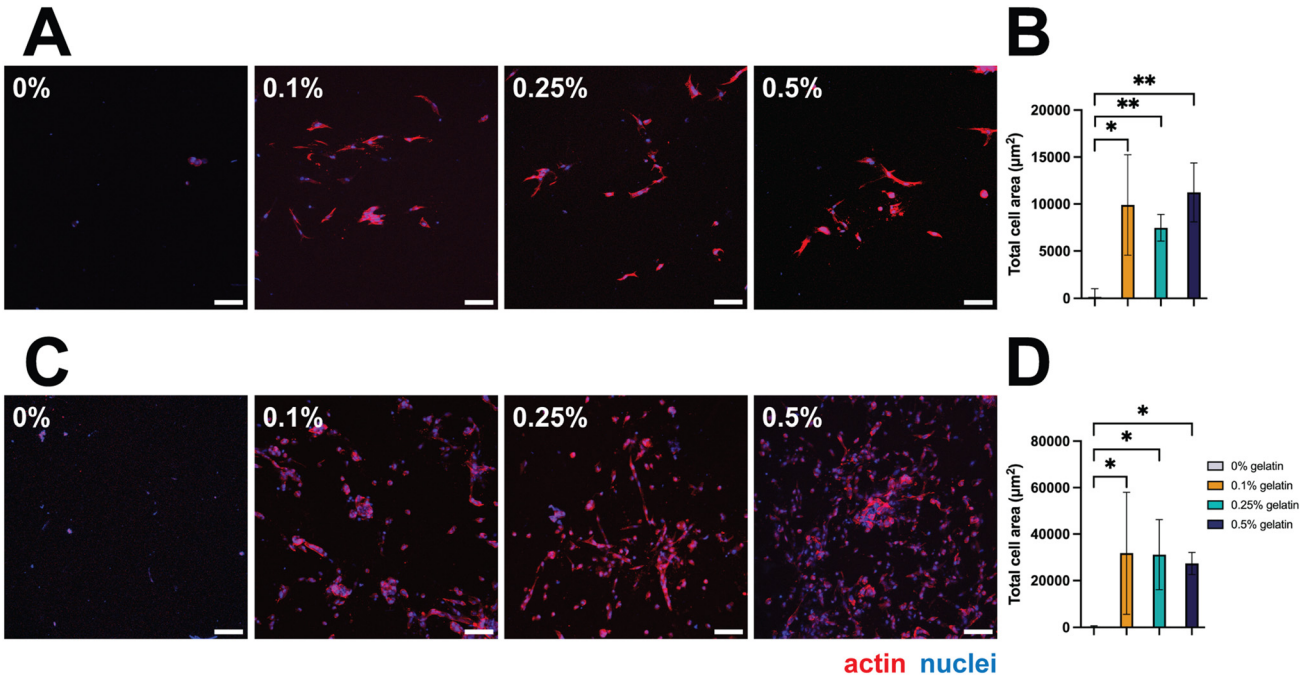

Fig. 6 Increased gelatin concentration in AcHyA hydrogels enhances HDF and iEC adhesion, spreading, and network formation, with 0.5% gelatin showing optimal cell behaviour. Hydrogels with 0%, 0.1%, 0.25%, and 0.5% gelatin were cultured with HDFs and iECs. (A) Images of HDFs and (C) images of iECs, after 7 days in culture, (B) cumulative cell area of HDFs, and (D) cumulative cell area of iECs. Scale bar is 100 μm. Data represents mean ± SD (n = 3). Analysis performed using one-way ANOVA; *p < 0.05, **p < 0.01.

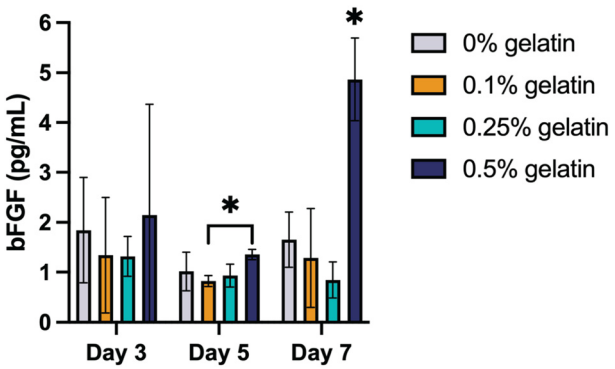

Fig. 7 Increased gelatin concentration in AcHyA hydrogels enhances bFGF expression over time in HDFs. bFGF expression was quantified in the supernatant collected at regular intervals from the HDF-seeded AcHyA hydrogels. Data represents mean ± SD (n = 3). Analysis performed using two-way ANOVA; *p < 0.05.

demonstrating that the incorporation of bioactive components like gelatin significantly improves cell adhesion to AcHyA hydrogels of similar biophysical properties.[25] Specifically, the enhanced bFGF secretion observed in the 0.5% gelatin group underscores the role of gelatin in promoting cellular engagement with the hydrogel matrix. The 0.5% gelatin formulation was identified as optimal for supporting the adhesion and spreading of both HDFs and iECs, with minimal impact on the structural characteristics of the AcHyA hydrogel network. This formulation was chosen for further functionalisation, including the incorporation of the AMP PP4-3.1.

As shown in Fig. S2,† tethering the AMP PP4-3.1 onto the hydrogel did not affect the biocompatibility of the latter and maintained support for the adhesion and spreading of both HDFs (Fig. S2A†) and iECs (Fig. S2B†) cells. In terms of biophysical properties, the incorporation of PP4-3.1 into AcHyA hydrogels did not affect their storage modulus (Fig. S3A†), swelling behaviour (Fig. S3B†) or stability across pH levels 6, 7, and 8 (Fig. S4A–C†). However, the peptide-grafted hydrogel showed slower enzymatic degradation at neutral and alkaline pH, likely due to electrostatic interactions of the peptide with HyA that stabilised the hydrogel network, reducing enzyme access to cleavage sites (Fig. S4D–F†).[88,89]

After confirming the biocompatibility of the AcHyA-AMP hydrogel, we investigated the antimicrobial activity of AcHyA-AMP conjugate against Gram-positive bacterium *Staphylococcus aureus* and Gram-negative bacterium *Escherichia coli*. *S. aureus* and *E. coli* are common pathogens associated with chronic wounds such as DFUs, often complicating wound healing and increasing infection risk.[46,49,100,101] Both bacteria contribute to persistent inflammation and delayed healing in chronic wounds like DFUs, highlighting the need for effective antimicrobial treatments. The antimicrobial potential of AcHyA-AMP conjugate was evaluated using optical density (OD) measurements at 600 nm and culture on agar plates.[59] Bacterial suspensions were incubated with either HyA, AcHyA, or AcHyA-AMP for 12 and 24 hours. In the presence of *S. aureus*, OD_{600} measurements at 12 hours revealed significant differences in bacterial growth. The OD_{600} for unmodified HyA reached 0.106 ± 0.004, while AcHyA showed a similar value of 0.120 ± 0.002, with no statistically significant difference between the two. In contrast, the OD_{600} for the AcHyA-AMP conjugate was markedly lower at 0.065 ± 0.010. After 24 h, the same trend was observed: OD_{600} values for HyA and AcHyA increased to 0.172 ± 0.008 and 0.157 ± 0.008, respectively, while AcHyA-AMP remained low at 0.069 ± 0.019 (Fig. 8A). To further validate these findings, the resulting solutions (at 24 h) were cultured on agar plates for an additional 24 h. No bacterial colonies formed on the plates treated with the AcHyA-AMP conjugate, contrasting with those treated with HyA and AcHyA, which were covered with bacterial colonies (Fig. 8B). These results suggest that while HyA and AcHyA exhibit a bacteriostatic effect by inhibiting bacterial growth in suspension, AcHyA-AMP demonstrates a bactericidal effect by killing the bacteria.

This antimicrobial activity of AcHyA-AMP was also assessed against *E. coli*. At 12 and 24 h, AcHyA-AMP exhibited higher OD_{600} values (0.084 ± 0.032 and 0.084 ± 0.050) compared to HyA (0.000 ± 0.000 at both time points) and AcHyA (0.001 ± 0.001 and 0.005 ± 0.004) (Fig. 8C). However, despite this apparent increase in OD, no bacterial colonies were recovered from the AcHyA-AMP-treated suspension when plated on agar (Fig. 8D). In contrast, both HyA and AcHyA conditions yielded substantial colony growth (Fig. 8D). Similar to *S. aureus*, the low OD_{600} values observed with HyA and AcHyA indicate a bacteriostatic effect, while the absence of viable colonies with AcHyA-AMP suggests a bactericidal action. The discrepancy between OD_{600} measurements and plating results for AcHyA-AMP likely reflects the presence of cellular debris from membrane disruption and lysis rather than bacterial proliferation.

These findings align with the expected mechanism of action of PP4-3.1 (the AMP used in this study), which exerts antimicrobial effects through direct interactions with bacterial membranes, leading to structural perturbation and cell death. While HyA alone appears to have bacteriostatic effects, as evidenced by the inhibition of bacterial growth in suspension, bacteria were still viable on agar, indicating that HyA alone does not kill bacteria. However, the direct conjugation of the AMP PP4-3.1 to the AcHyA results in the absence of viable bacteria on agar, confirming the bactericidal nature of the AcHyA-AMP conjugate. This study demonstrates a marked increase in the antimicrobial activity of HyA following conjugation of the AMP PP4-3.1, as evidenced by its antimicrobial action against both *S. aureus* and *E. coli*. Since the AMP is covalently bound to AcHyA and no hyaluronidase is present in the system, it is unlikely that its antimicrobial activity arises from passive peptide release into the surrounding media. Instead, the observed effect is presumably due to direct contact between the bacteria and the conjugated AMP, where localised interactions with the bacterial membranes lead to disruption and cell death. Indeed, AMPs primarily exert their antimicrobial action through bacterial membrane perturbation

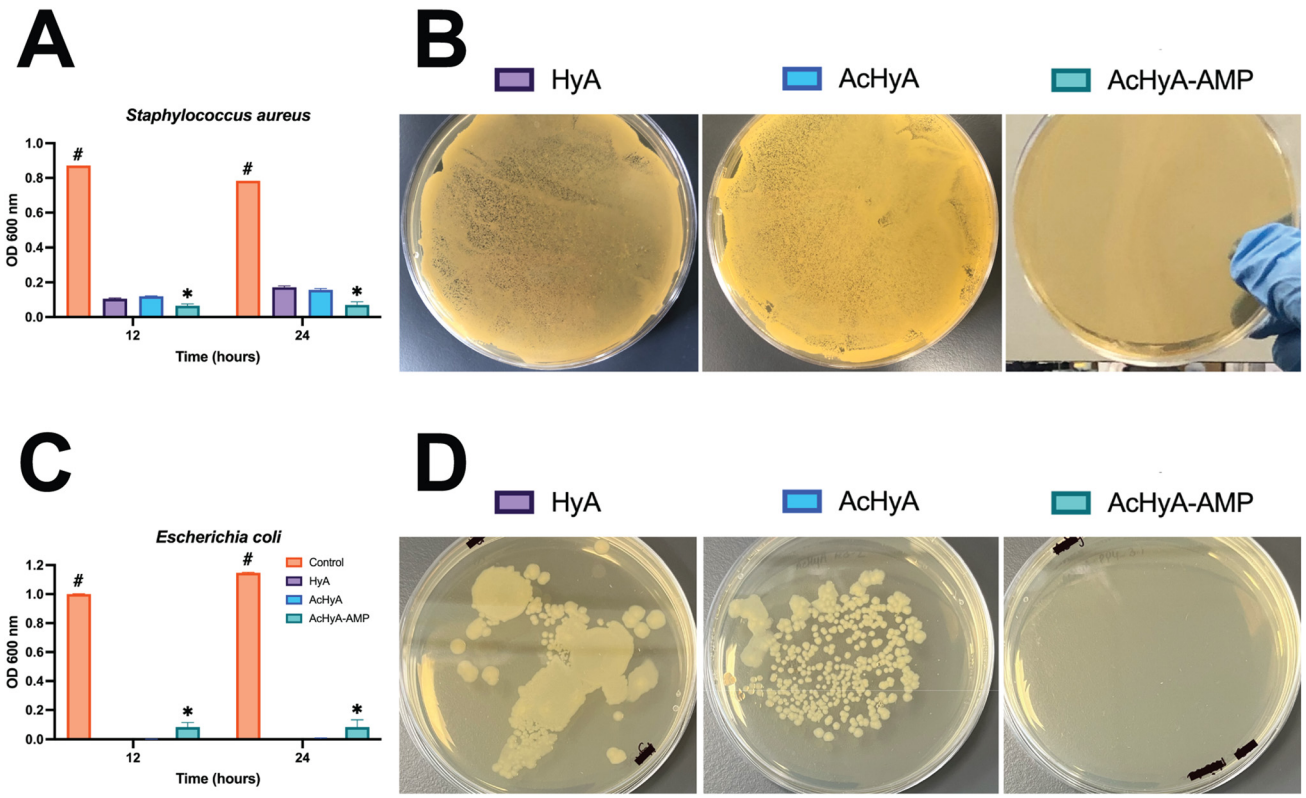

Fig. 8 AcHyA-AMP conjugates demonstrate significant bactericidal activity against *S. aureus* and *E. coli*, compared to unmodified HyA and AcHyA. The PP4-3.1 AMP was conjugated to AcHyA-G, and the antimicrobial activity of the AcHyA-AMP conjugate was evaluated by (A) OD_{600} measurements and (B) colony formation after an additional 24 h for *S. aureus*, and (C) OD_{600} measurements and (D) colony formation after an additional 24 h for *E. coli*. Data represent mean ± SD (n = 3). Analysis performed using two-way ANOVA. * indicates statistical differences between groups, and # indicates difference *versus* the control group. *$p < 0.001$, #$p < 0.001$.

or disruption, leading to cell lysis.[102,103] In line with this, peptide 3.1 – a cationic, amphipathic, α-helical AMP, has been reported to hypothetically exert its antimicrobial effect by perturbing bacterial membranes, potentially through pore-forming and/or carpet-like mechanisms.[104] Previous studies by Gomes *et al.* demonstrated the effectiveness of the selected AMP, PP4-3.1, against both Gram-positive and Gram-negative bacteria. PP4-3.1 is a hybrid peptide, combining the sequence of the cosmeceutical pentapeptide-4 (PP4) with that of a reported AMP named 3.1.[45] Furthermore, PP4-3.1 exhibits MIC values lower than those of most recently reported peptide-based antimicrobials.[45]

In this study, the AMP was covalently immobilised onto AcHyA *via* acrylate–thiol Michael addition through the incorporation of a spacer (Ahx) and a cysteine residue. This covalent attachment enhances the AMP's stability and ensures its localisation at the infection site, enabling continuous neutralisation of pathogens and enhanced antimicrobial efficacy over time.[42–44] This immobilisation offers several advantages, including reduced peptide aggregation, slower degradation, and enhanced antimicrobial efficacy by maintaining high local concentrations at the hydrogel surface.[105] By restricting peptide diffusion, immobilisation optimises its ability to interact with bacterial membranes, which is crucial for sustained antimicrobial action. Unlike free peptides, which can translocate across membranes and target intracellular sites, immobilised peptides primarily exert their antimicrobial effects through surface-driven membrane disruption.[106] The presence of the spacer (Ahx) preserves the peptide's amphipathic properties, facilitating its interaction with bacterial membranes, leading to membrane perturbation and subsequent cell lysis.[107] This mechanism may also involve changes in bacterial surface electrostatics, where the high concentration of positively charged peptides potentially displaces counterions from the membrane, triggering autolytic enzyme activation and disrupting ionic balance in deeper membrane layers.[106]

The conjugation of AMP PP4-3.1 into AcHyA hydrogels offers a promising strategy for preventing and treating bacterial infections in chronic wounds. By ensuring the peptide's localisation at infection sites, AcHyA-AMP provides continuous pathogen neutralisation, reducing systemic exposure, thereby reducing any potential side effects. Interestingly, HyA itself has been reported to have antimicrobial properties.[108–110] This has been attributed to an ability to disrupt bacterial adhesion and biofilm formation, sequestering essential ions needed for bacterial survival and proliferation, and hindering colonisation through its highly hydrophilic and hydrogel-like properties, which create a physical barrier.[108,110,111] Here, the HyA matrix

may contribute to the antimicrobial activity by localising bacteria at the AcHyA-AMP conjugate interface, facilitating sustained peptide-bacteria interactions. Our results support the hypothesis that the AMP's antimicrobial activity arises from direct interactions with bacterial membranes, causing membrane destabilisation and cell death. The combined effect of the AMP's electrostatic and hydrophobic interactions, as well as its high local concentration, underscores the potential of AcHyA-AMP conjugates as a potent antimicrobial treatment for chronic wound infections, providing a new approach to improving wound healing and infection management.

Conclusion

We have developed and characterised AcHyA hydrogels functionalised with both gelatin and PP4-3.1 peptide to enhance cell adhesion while providing antimicrobial activity for the treatment of chronic wounds. The addition of gelatin and the AMP was achieved without compromising the biophysical and mechanical properties of the AcHyA hydrogels, which retained their structural integrity and mechanical stability. Gelatin incorporation enhanced swelling behaviour and provided a favourable environment for cellular activity, namely by supporting the adhesion and spreading of HDFs and iECs, with the 0.5% gelatin concentration showing the highest bioactivity. This formulation also promoted fibroblast activation, as evidenced by increased secretion of bFGF, a key growth factor involved in tissue regeneration and angiogenesis. The sustained bFGF production observed in the 0.5% gelatin hydrogel suggests that this formulation supports long-term fibroblast engagement, which may contribute to improved wound healing outcomes. Meanwhile, the conjugation of the AMP PP4-3.1 delivered an AcHyA formulation with bactericidal action on *S. aureus* and *E. coli*, two of the most prevalent bacterial pathogens in chronic wounds. Thus, this gelatin and peptide-tethered AcHyA hydrogel demonstrates a local antimicrobial effect, providing a protective barrier against infection while supporting cell adhesion. Given the challenges associated with chronic wound healing, these AcHyA hydrogels, decorated with ECM moieties and AMPs, represent a promising strategy to reduce infection and accelerate recovery in chronic wounds. Future research will involve evaluation in pre-clinical wound models to further assess the efficacy and long-term potential of gelatin and AMP-decorated AcHyA hydrogels in promoting wound healing.

Data availability

Data from this study is available from OSF Repository at [https://osf.io/3tyrd/?view_only=950a75755918493395395b93c57fa02e].

Conflicts of interest

There are no conflicts to declare.

Acknowledgements

This work received support from The European Federation for the Study of Diabetes/Lily European Diabetes Research Programme, Research Ireland – Grant Number 13/RC/2073_P2, and co-funded by the European Union (EU) under MedTrain + Grant Agreement No. 101081457.

Thanks are further due to Fundação para a Ciência e a Tecnologia (FCT, Portugal) for funding through project 2023.12331.PEX. The authors would like to thank Dr Brenton Cavanagh for his valuable contributions and technical support for microscopy.

References

1 V. Falanga, R. R. Isseroff, A. M. Soulika, M. Romanelli, D. Margolis, S. Kapp, M. Granick and K. Harding, *Nat. Rev. Dis. Primers*, 2022, **8**, 50.
2 K. Raziyeva, Y. Kim, Z. Zharkinbekov, K. Kassymbek, S. Jimi and A. Saparov, *Biomolecules*, 2021, **11**, 700.
3 L. Martinengo, M. Olsson, R. Bajpai, M. Soljak, Z. Upton, A. Schmidtchen, J. Car and K. Järbrink, *Ann. Epidemiol.*, 2019, **29**, 8–15.
4 M. Piipponen, D. Li and N. X. Landén, *Int. J. Mol. Sci.*, 2020, **21**, 8790.
5 R. Zhao, H. Liang, E. Clarke, C. Jackson and M. Xue, *Int. J. Mol. Sci.*, 2016, **17**, 2085.
6 R. G. Frykberg and J. Banks, *Adv. Wound Care*, 2015, **4**, 560–582.
7 E. Darwin and M. Tomic-Canic, *Curr. Dermatol. Rep..*, 2018, **7**, 296–302.
8 S. A. Eming, P. Martin and M. Tomic-Canic, *Sci. Transl. Med.*, 2014, **6**, 265sr6–265sr6.
9 U. Okonkwo and L. DiPietro, *Int. J. Mol. Sci.*, 2017, **18**, 1419.
10 L. Hosty, T. Heatherington, F. Quondamatteo and S. Browne, *Mol. Biol. Rep.*, 2024, **51**, 830.
11 M. G. Monaghan, R. Borah, C. Thomsen and S. Browne, *Adv. Drug Delivery Rev.*, 2023, **203**, 115120.
12 S. Browne, N. Petit and F. Quondamatteo, *Cell Tissue Res.*, 2024, **395**, 133–145.
13 E. Caló and V. V. Khutoryanskiy, *Eur. Polym. J.*, 2015, **65**, 252–267.
14 S. Correa, A. K. Grosskopf, H. Lopez Hernandez, D. Chan, A. C. Yu, L. M. Stapleton and E. A. Appel, *Chem. Rev.*, 2021, **121**, 11385–11457.
15 H. P. Felgueiras, *Pharmaceutics*, 2023, **15**, 258.
16 S. Browne and K. E. Healy, *Adv. Drug Delivery Rev.*, 2019, **146**, 155–169.
17 J. A. Burdick and G. D. Prestwich, *Adv. Mater.*, 2011, **23**, H41–H56.
18 G. D. Prestwich, *J. Controlled Release*, 2011, **155**, 193–199.
19 N. Petit, Y. J. Chang, F. A. Lobianco, T. Hodgkinson and S. Browne, *Mater. Today Bio*, 2025, **31**, 101596.
20 E. L. Pardue, S. Ibrahim and A. Ramamurthi, *Organogenesis*, 2008, **4**, 203–214.

21 D. Park, Y. Kim, H. Kim, K. Kim, Y.-S. Lee, J. Choe, J.-H. Hahn, H. Lee, J. Jeon, C. Choi, Y.-M. Kim and D. Jeoung, *Mol. Cells*, 2012, **33**, 563–574.
22 H. P. Lorenz and N. S. Adzick, *West. J. Med.*, 1993, **159**, 350–355.
23 S. Browne, A. K. Jha, K. Ameri, S. G. Marcus, Y. Yeghiazarians and K. E. Healy, *PLoS One*, 2018, **13**, e0194679.
24 A. K. Jha, K. M. Tharp, S. Browne, J. Ye, A. Stahl, Y. Yeghiazarians and K. E. Healy, *Biomaterials*, 2016, **89**, 136–147.
25 S. Browne, S. Hossainy and K. Healy, *ACS Biomater. Sci. Eng.*, 2020, **6**, 1135–1143.
26 A. K. Jha, A. Mathur, F. L. Svedlund, J. Ye, Y. Yeghiazarians and K. E. Healy, *J. Controlled Release*, 2015, **209**, 308–316.
27 J. Kim, Y. Park, G. Tae, K. B. Lee, C. M. Hwang, S. J. Hwang, I. S. Kim, I. Noh and K. Sun, *J. Biomed. Mater. Res., Part A*, 2009, **88A**, 967–975.
28 M. N. Collins and C. Birkinshaw, *Carbohydr. Polym.*, 2013, **92**, 1262–1279.
29 J. A. Burdick and G. D. Prestwich, *Adv. Mater.*, 2011, **23**, H41–H56.
30 J. K. Kim, Y. Xu, X. Xu, D. R. Keene, S. Gurusiddappa, X. Liang, K. K. Wary and M. Höök, *J. Biol. Chem.*, 2005, **280**, 32512–32520.
31 H. Wang, O. C. Boerman, K. Sariibrahimoglu, Y. Li, J. A. Jansen and S. C. G. Leeuwenburgh, *Biomaterials*, 2012, **33**, 8695–8703.
32 W.-M. Zhang, J. Käpylä, J. S. Puranen, C. G. Knight, C.-F. Tiger, O. T. Pentikäinen, M. S. Johnson, R. W. Farndale, J. Heino and D. Gullberg, *J. Biol. Chem.*, 2003, **278**, 7270–7277.
33 S. Guo and L. A. DiPietro, *J. Dent. Res.*, 2010, **89**, 219–229.
34 K. Rahim, S. Saleha, X. Zhu, L. Huo, A. Basit and O. L. Franco, *Microb. Ecol.*, 2017, **73**, 710–721.
35 J. Murugaiyan, P. A. Kumar, G. S. Rao, K. Iskandar, S. Hawser, J. P. Hays, Y. Mohsen, S. Adukkadukkam, W. A. Awuah, R. A. M. Jose, N. Sylvia, E. P. Nansubuga, B. Tilocca, P. Roncada, N. Roson-Calero, J. Moreno-Morales, R. Amin, B. K. Kumar, A. Kumar, A.-R. Toufik, T. N. Zaw, O. O. Akinwotu, M. P. Satyaseela and M. B. M. Van Dongen, *Antibiotics*, 2022, **11**, 200.
36 M. McGrath, K. Zimkowska, K. J. Genoud, J. Maughan, J. Gutierrez Gonzalez, S. Browne and F. J. O'Brien, *ACS Appl. Mater. Interfaces*, 2023, **15**, 17444–17458.
37 A. Gomes, L. J. Bessa, I. Fernandes, R. Ferraz, N. Mateus, P. Gameiro, C. Teixeira and P. Gomes, *Front. Microbiol.*, 2019, **10**, 1915.
38 C. Ghosh, P. Sarkar, R. Issa and J. Haldar, *Trends Microbiol.*, 2019, **27**, 323–338.
39 G. S. Dijksteel, M. M. W. Ulrich, E. Middelkoop and B. K. H. L. Boekema, *Front. Microbiol.*, 2021, **12**, 616979.
40 M. L. Mangoni, A. M. McDermott and M. Zasloff, *Exp. Dermatol.*, 2016, **25**, 167–173.
41 P. M. Alves, C. C. Barrias, P. Gomes and M. C. L. Martins, *Acta Biomater.*, 2024, **181**, 98–116.
42 J. W. Soares, R. Kirby, L. A. Doherty, A. Meehan and S. Arcidiacono, *J. Pept. Sci.*, 2015, **21**, 669–679.
43 B. Skerlavaj and G. Boix-Lemonche, *Antibiotics*, 2023, **12**, 211.
44 V. Patrulea, G. Borchard and O. Jordan, *Pharmaceutics*, 2020, **12**, 840.
45 A. Gomes, L. J. Bessa, I. Fernandes, R. Ferraz, C. Monteiro, M. C. L. Martins, N. Mateus, P. Gameiro, C. Teixeira and P. Gomes, *Pharmaceutics*, 2021, **13**, 1962.
46 S. Jain and R. Barman, *Indian J. Endocrinol. Metab.*, 2017, **21**, 688.
47 K. E. Macdonald, S. Boeckh, H. J. Stacey and J. D. Jones, *BMC Infect. Dis.*, 2021, **21**, 770.
48 R. Edwards and K. G. Harding, *Curr. Opin. Infect. Dis.*, 2004, 91–96.
49 M. Idrees, I. Khan, A. Ullah, S. M. M. Shah, H. Ullah, M. A. Khan, R. Almeer, Z. A. Shah and T. Nadeem, *J. King Saud Univ., Sci.*, 2024, **36**, 103320.
50 S. L. Natividad-Diaz, S. Browne, A. K. Jha, Z. Ma, S. Hossainy, Y. K. Kurokawa, S. C. George and K. E. Healy, *Biomaterials*, 2019, **194**, 73–83.
51 N. Petit, J. M. Dyer, J. A. Gerrard, L. J. Domigan and S. Clerens, *BBA Adv.*, 2023, **3**, 100086.
52 M. Kurisawa, J. E. Chung, Y. Y. Yang, S. J. Gao and H. Uyama, *Chem. Commun.*, 2005, 4312.
53 J. Schindelin, I. Arganda-Carreras, E. Frise, V. Kaynig, M. Longair, T. Pietzsch, S. Preibisch, C. Rueden, S. Saalfeld, B. Schmid, J.-Y. Tinevez, D. J. White, V. Hartenstein, K. Eliceiri, P. Tomancak and A. Cardona, *Nat. Methods*, 2012, **9**, 676–682.
54 K. Y. Lee, J. A. Rowley, P. Eiselt, E. M. Moy, K. H. Bouhadir and D. J. Mooney, *Macromolecules*, 2000, **33**, 4291–4294.
55 J. E. Mark and B. Erman, *Rubberlike elasticity: a molecular primer*, Cambridge University Press, 2007.
56 E. I. Altiok, J. L. Santiago-Ortiz, F. L. Svedlund, A. Zbinden, A. K. Jha, D. Bhatnagar, P. Loskill, W. M. Jackson, D. V. Schaffer and K. E. Healy, *Biomaterials*, 2016, **93**, 95–105.
57 S. J. De Jong, B. Van Eerdenbrugh, C. F. Van Nostrum, J. J. Kettenes-van Den Bosch and W. E. Hennink, *J. Controlled Release*, 2001, **71**, 261–275.
58 D. M. Soumpasis, *Biophys. J.*, 1983, **41**, 95–97.
59 J. Zhou, H. Zhang, M. S. Fareed, Y. He, Y. Lu, C. Yang, Z. Wang, J. Su, P. Wang, W. Yan and K. Wang, *ACS Nano*, 2022, **16**, 7636–7650.
60 Agilent, *E. coli* Cell Culture Concentration from OD600 Calculator, **https://www.agilent.com/store/biocalculators/calcODBacterial.jsp**, (accessed March 3, 2025).
61 N. Ahmad, S. N. A. Bukhari, M. A. Hussain, H. Ejaz, M. U. Munir and M. W. Amjad, *RSC Adv.*, 2024, **14**, 13535–13564.
62 A. Copling, M. Akantibila, R. Kumaresan, G. Fleischer, D. Cortes, R. S. Tripathi, V. J. Carabetta and S. L. Vega, *Int. J. Mol. Sci.*, 2023, **24**, 7563.

63 E. R. Cross, S. M. Coulter, S. Pentlavalli and G. Laverty, *Soft Matter*, 2021, **17**, 8001–8021.
64 Y. Guo, F. Gao, M. Rafiq, B. Yu, H. Cong and Y. Shen, *Int. J. Biol. Macromol.*, 2024, **274**, 133494.
65 C. Liang, H. Wang, Z. Lin, C. Zhang, G. Liu and Y. Hu, *Front. Bioeng. Biotechnol.*, 2023, **11**, 1310349.
66 E. G. Wiita, Z. Toprakcioglu, A. K. Jayaram and T. P. J. Knowles, *ACS Appl. Mater. Interfaces*, 2024, **16**, 46167–46176.
67 D. P. Nair, M. Podgórski, S. Chatani, T. Gong, W. Xi, C. R. Fenoli and C. N. Bowman, *Chem. Mater.*, 2014, **26**, 724–744.
68 J. Zhu, *Biomaterials*, 2010, **31**, 4639–4656.
69 X. Kong, Q. Tang, X. Chen, Y. Tu, S. Sun and Z. Sun, *Neural Regener. Res.*, 2017, **12**, 1003.
70 Z. Xiao, S. Zhao, X. Zhang, G. Wei and Z. Su, *Macromol. Mater. Eng.*, 2022, **307**, 2200385.
71 S. Tao, S. Zhang, K. Wei, K. Maniura-Weber, Z. Li and Q. Ren, *Adv. Healthcare Mater.*, 2024, 2400921.
72 L. I. F. Moura, A. M. A. Dias, E. Carvalho and H. C. De Sousa, *Acta Biomater.*, 2013, **9**, 7093–7114.
73 R. Yang, X. Liu, Y. Ren, W. Xue, S. Liu, P. Wang, M. Zhao, H. Xu and B. Chi, *Acta Biomater.*, 2021, **127**, 102–115.
74 D. C. West, I. N. Hampson, F. Arnold and S. Kumar, *Science*, 1985, **228**, 1324–1326.
75 H. Yang, L. Song, Y. Zou, D. Sun, L. Wang, Z. Yu and J. Guo, *ACS Appl. Bio Mater.*, 2021, **4**, 311–324.
76 K. L. Aya and R. Stern, *Wound Repair Regen.*, 2014, **22**, 579–593.
77 J. L. West and J. A. Hubbell, *Macromolecules*, 1999, **32**, 241–244.
78 J. Xia, Z.-Y. Liu, Z.-Y. Han, Y. Yuan, Y. Shao, X.-Q. Feng and D. A. Weitz, *Acta Biomater.*, 2022, **141**, 178–189.
79 N. Raina, R. Pahwa, J. Bhattacharya, A. K. Paul, V. Nissapatorn, M. de Lourdes Pereira, S. M. R. Oliveira, K. G. Dolma, M. Rahmatullah, P. Wilairatana and M. Gupta, *Pharmaceutics*, 2022, **14**, 574.
80 B. Liu and K. Chen, *Gels*, 2024, **10**, 262.
81 M. S. Rehmann, K. M. Skeens, P. M. Kharkar, E. M. Ford, E. Maverakis, K. H. Lee and A. M. Kloxin, *Biomacromolecules*, 2017, **18**, 3131–3142.
82 E. Hoch, C. Schuh, T. Hirth, G. E. M. Tovar and K. Borchers, *J. Mater. Sci.: Mater. Med.*, 2012, **23**, 2607–2617.
83 B. Ananthanarayanan, Y. Kim and S. Kumar, *Biomaterials*, 2011, **32**, 7913–7923.
84 M. N. Collins and C. Birkinshaw, *J. Appl. Polym. Sci.*, 2008, **109**, 923–931.
85 K. Braeckmans, L. Peeters, N. N. Sanders, S. C. De Smedt and J. Demeester, *Biophys. J.*, 2003, **85**, 2240–2252.
86 J. E. Mealy, C. B. Rodell and J. A. Burdick, *J. Mater. Chem. B*, 2015, **3**, 8010–8019.
87 J. Parlow, A. Rodler, J. Gråsjö, H. Sjögren and P. Hansson, *Int. J. Pharm.*, 2024, **664**, 124628.
88 Q. Luo, J. W. Borst, A. H. Westphal, R. M. Boom and A. E. M. Janssen, *Food Hydrocolloids*, 2017, **66**, 318–325.
89 N. Petit, J. M. Dyer, M. Richena, L. J. Domigan, J. A. Gerrard and S. Clerens, *Int. J. Food Sci. Technol.*, 2024, **59**, 2927–2942.
90 S. G. Zambuto, S. S. Kolluru, E. Ferchichi, H. F. Rudewick, D. M. Fodera, K. M. Myers, S. P. Zustiak and M. L. Oyen, *J. Mech. Behav. Biomed. Mater.*, 2024, **154**, 106509.
91 P. Dhavalikar, A. Robinson, Z. Lan, D. Jenkins, M. Chwatko, K. Salhadar, A. Jose, R. Kar, E. Shoga, A. Kannapiran and E. Cosgriff-Hernandez, *Adv. Healthcare Mater.*, 2020, **9**, 2000795.
92 J. Karam, B. J. Singer, H. Miwa, L. H. Chen, K. Maran, M. Hasani, S. Garza, B. Onyekwere, H.-C. Yeh, S. Li, D. D. Carlo and S. K. Seidlits, *Acta Biomater.*, 2023, **169**, 228–242.
93 T. Yeung, P. C. Georges, L. A. Flanagan, B. Marg, M. Ortiz, M. Funaki, N. Zahir, W. Ming, V. Weaver and P. A. Janmey, *Cell Motil. Cytoskeleton*, 2005, **60**, 24–34.
94 J. Li, Y. Zhang and R. S. Kirsner, *Microsc. Res. Tech.*, 2003, **60**, 107–114.
95 X. Zhang, X. Kang, L. Ji, J. Bai, W. Liu and Z. Wang, *Int. J. Nanomed.*, 2018, **13**, 3897–3906.
96 S. Kanazawa, T. Fujiwara, S. Matsuzaki, K. Shingaki, M. Taniguchi, S. Miyata, M. Tohyama, Y. Sakai, K. Yano, K. Hosokawa and T. Kubo, *PLoS One*, 2010, **5**, e12228.
97 S. Ouasti, P. J. Kingham, G. Terenghi and N. Tirelli, *Biomaterials*, 2012, **33**, 1120–1134.
98 G. Camci-Unal, D. Cuttica, N. Annabi, D. Demarchi and A. Khademhosseini, *Biomacromolecules*, 2013, **14**, 1085–1092.
99 S. Poveda-Reyes, V. Moulisova, E. Sanmartín-Masiá, L. Quintanilla-Sierra, M. Salmerón-Sánchez and G. G. Ferrer, *Macromol. Biosci.*, 2016, **16**, 1311–1324.
100 F. L. Sapico, J. L. Witte, H. N. Canawati, J. Z. Montgomerie and A. N. Bessman, *Clin. Infect. Dis.*, 1984, **6**, S171–S176.
101 N. Djahmi, N. Messad, S. Nedjai, A. Moussaoui, D. Mazouz, J.-L. Richard, A. Sotto and J.-P. Lavigne, *Clin. Microbiol. Infect.*, 2013, **19**, E398–E404.
102 Y. Luo and Y. Song, *Int. J. Mol. Sci.*, 2021, **22**, 11401.
103 V. Nizet, *Curr. Issues Mol. Biol.*, 2006, **8**, 11–26.
104 S. Kang, H. Won, W. Choi and B. Lee, *J. Pept. Sci.*, 2009, **15**, 583–588.
105 F. Costa, I. F. Carvalho, R. C. Montelaro, P. Gomes and M. C. L. Martins, *Acta Biomater.*, 2011, **7**, 1431–1440.
106 B. Bechinger and S.-U. Gorr, *J. Dent. Res.*, 2017, **96**, 254–260.
107 S. Ghosh, S. Chatterjee and P. Satpati, *J. Chem. Inf. Model.*, 2023, **63**, 5823–5833.
108 A. Ardizzoni, R. G. Neglia, M. C. Baschieri, C. Cermelli, M. Caratozzolo, E. Righi, B. Palmieri and E. Blasi, *J. Mater. Sci.: Mater. Med.*, 2011, **22**, 2329–2338.
109 F. Zamboni, C. K. Wong and M. N. Collins, *Bioact. Mater.*, 2023, **19**, 458–473.
110 G. A. Carlson, J. L. Dragoo, B. Samimi, D. A. Bruckner, G. W. Bernard, M. Hedrick and P. Benhaim, *Biochem. Biophys. Res. Commun.*, 2004, **321**, 472–478.
111 P. Pirnazar, L. Wolinsky, S. Nachnani, S. Haake, A. Pilloni and G. W. Bernard, *J. Periodontol.*, 1999, **70**, 370–374.